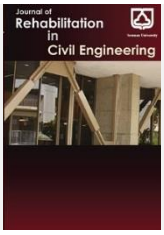

Journal of Rehabilitation in Civil Engineering

Journal homepage: https://civiljournal.semnan.ac.ir/

Sensitivity Analysis of Engineering Demand Parameters: Empirical and Analytical Approaches to Structural Loss Estimation

Roi Milyardi [1,*]; Krishna Suryanto Pribadi [2]; Muhamad Abduh [2]; Irwan Meilano [3]; Erwin Lim [4]; Reini Wirahadikusumah [2]; Patria Kusumaningrum [4]; Eliza Rosmaya Puri [5]

1. Ph.D. Candidate, Department of Civil Engineering, Institut Teknologi Bandung, Bandung, Indonesia
2. Professor, Faculty of Civil and Environmental Engineering, Institut Teknologi Bandung, Bandung, Indonesia
3. Professor, Faculty of Earth Science and Technology, Institut Teknologi Bandung, Bandung, Indonesia
4. Assistant Professor, Faculty of Civil and Environmental Engineering, Institut Teknologi Bandung, Bandung, Indonesia
5. Instructor, Faculty of Civil and Environmental Engineering, Institut Teknologi Bandung, Bandung, Indonesia

* Corresponding author: *35021012@mahasiswa.itb.ac.id*

ARTICLE INFO

Article history:
Received: 24 October 2024
Revised: 07 December 2024
Accepted: 14 January 2025

Keywords:
Structural loss estimation;
Fragility curve;
HAZUS;
School building;
Annualized earthquake losses.

ABSTRACT

Variations in the engineering demand parameter (EDP) of a region significantly affect the fragility curve, which is believed to impact the estimation of earthquake losses; hence, there is a need to adjust for different regional characteristics. In earthquake-prone regions that already have empirical EDP databases, fragility curve development generally uses this information. Regions without EDP databases require additional effort to start their development or adopt existing methods as a short-term solution. Some studies show that direct adoption is oblivious to the consequences of the resulting estimation deviations. This study investigates the effect of EDP variations derived from an analytical method—incremental dynamic analysis (IDA)—and two empirical methods—HAZUS and RISK-EU—on seismic loss estimation in typical school buildings in Bandung City, Indonesia. Three school buildings are used as case studies, with existing structural data collected through non-destructive testing on each building used for the analytical method. The observed earthquake losses are estimated in a single hazard scenario at eight return periods and in the form of annualized earthquake losses (AEL). The results of this study illustrate that the EDP variation has a significant impact on loss estimation based on the relative difference determined with the analytical method. The sensitivity analysis results indicate that the HAZUS method has a relative deviation of 2.61%–74.62% in the single hazard scenario and 19.66%–71.90% in the AEL, and the RISK-EU method shows a relative deviation of 3.48%–672.03% in the single hazard scenario and 53.44%–222.82% in the AEL. Simultaneously, the absolute deviation in the single hazard scenario shows that the HAZUS method has a deviation of <12%BRC (building replacement cost) and the RISK-EU method <15%BRC. The absolute deviation value can be utilized as a reference when considering directly adopting empirical methods in developing countries that do not have an EDP database.

E-ISSN: 2345-4423

How to cite this article: Milyardi, R., Pribadi, K.S., Abduh, M., Meilano, I., Lim, E., Wirahadikusumah, R. , Kusumaningrum, P. and Puri, E. Rosmaya (2025). Sensitivity Analysis of Engineering Demand Parameters: Empirical and Analytical Approaches to Structural Loss Estimation. Journal of Rehabilitation in Civil Engineering, 13(4), 25-46. https://doi.org/10.22075/jrce.2025.35649.2193

1. Introduction

Various methods have been developed to estimate earthquake losses in buildings, with one of the most prevalently used based on fragility curves. This method attempts to model various uncertainties in estimating losses into a probabilistic framework [1]. The most widely used analytical method for constructing earthquake fragility curves is incremental dynamic analysis (IDA). The approach employs a series of complex processes that require certain levels of expertise and resources (time and cost), particularly for investigating existing structures [2,3]. With its rigorous methods, IDA can provide reasonably accurate damage probabilities based on detailed building data [4]. However, alternative approaches to the rigorous IDA method exist, such as the Hazards-United States (HAZUS) and RISK-EU WP4 methods, which develop fragility curve models using empirical methods. This helps reduce the complexity of fragility curve modeling. Each method requires a minimum amount of data (location, structure type, and floor height) in its input process [5,6].

The HAZUS method was developed by the Federal Emergency Management Agency in 1992 to provide loss estimations following possible earthquakes. The RISK-EU WP4 method was devised by the European Commission in 2003. Both methods use simplified processes to generate capacity and fragility curves by providing engineering demand parameters (EDPs) grouped by structure type and number of floors [7]. The EDPs are organized by building type in each region [8,9].

The fragility curve output in the form of the probability of building damage at each level of damage is utilized to determine earthquake loss estimation [10,11]. The probability value, which is influenced by the capacity of the structure and the hazard scenario, is a variable sensitive to the amount of loss estimation [12]. In a single hazard scenario, the loss estimation value can provide information on the amount of loss; however, in the case of risk transfer strategy, such as determining insurance premiums, an annualized earthquake losses (AEL) value is required. The value is calculated using various hazard scenario return periods to represent the annualized risk. In addition, AEL can be used as a decision-making and risk assessment instrument by authorities in the disaster mitigation process [13,14].

Bandung City, West Java Province, one of the most populous cities, has active fault-related earthquake hazards [15–17]. One such earthquake threat is the Lembang fault, an active fault located north of the city, with the potential to cause a 6.5–7.0 Mw earthquake [18]. School buildings are the public facilities most affected by earthquake damage, according to national historical data [19]. The extent of damage depends on the condition of the school buildings at the time of the disaster; approximately 86.41% of damage ranges from light to severe, based on national scale data [20]. In Bandung, according to a study on the distribution of structure type, the concrete moment frame (C1) was the most dominant (72.46%), with variations in the levels of code from the local building code [21]. In addition to the type of structure, building codes related to earthquake loads and building structures in Indonesia can be classified into three levels: low-code, moderate-code, and high-code [22,23]. In CR structure-type buildings, low-code includes buildings built before 1991, moderate-code encompasses buildings constructed between 1991 and 2012, and high-code includes buildings built after 2012 [23]. Despite being an earthquake-prone area, research related to loss estimation in the Indonesian region, especially Bandung, is still sparse, particularly regarding the vulnerability of buildings and the development of disaster loss estimation models [24]. This can hinder the strategy to improve resilience, especially in finance, through the poor availability of earthquake-loss data. The most feasible of the existing approaches are empirical techniques

(HAZUS and RISK-EU), as the IDA method is extremely challenging to adopt with the limited availability of school building data. Previous studies have showcased confidence in the direct adoption of empirical methods in different regions [25–30]. However, these studies have not identified how large the estimation deviation is when adopting the direct loss estimation method. Identifying the deviation is necessary for the process of choosing the direct adoption option.

This study investigates the effect of EDP variations derived from an analytical method (IDA) and two empirical methods (HAZUS and RISK-EU) on seismic loss estimation in typical school buildings in Bandung City, Indonesia. Sensitivity analysis can provide better validation of the adoption process and an idea of the deviation amount of the estimated value as a consequence of adopting the methods. The study focuses on the C1 structure and its replacement cost. The IDA and pushover methods are used as benchmarks for empirical methods, as the study involves a comprehensive analysis requiring detailed data [31]. A field survey of the case study buildings was also conducted for this comparative study with IDA. This study compares the EDP usage of the existing HAZUS and RISK-EU methods to the characteristics of structures in Indonesia through school-building case studies. The comparative study can be used as a reference for the process of adopting the methods in Indonesia. The research findings are aligned with the UN Sustainable Development Goals (SDGs), specifically contributing to expanding the application of earthquake loss estimation, directly in line with UN SDG Target 11.5.2: "the application of direct economic losses attributed to disasters in relation to gross domestic product (GDP) by 2030." This is part of the related goal "Disaster Risk Reduction" in Goal 11, which states, "Make cities and human settlements inclusive, safe, resilient and sustainable." Sections 2 and 3 describe the literature review related to the fragility curve and loss estimation conducted to achieve the objectives of this study.

2. Review of fragility curve analysis procedure

This chapter comprises a literature study on the fragility curve in the empirical and analytical methods conducted as part of the process of estimating structural losses due to earthquakes.

2.1. Empirical methods (HAZUS and RISK-EU methodologies)

The HAZUS method of earthquake loss estimation in General Building Stock (GBS) can estimate various kinds of earthquake losses, such as direct costs for repair and replacement, loss of function and restoration times, and extent of induced hazards [7]. In GBS, generic EDP consists of a generic building capacity and fragility function classified by a building lateral force resisting system, height, level of code, and occupancy. The EDP provides structural response, damage, and repair costs as an output. Figure 1 presents the building structural damage estimation process used in HAZUS; it is explained in detail below. For the hazard component, the potential Earth science hazards associated with ground motion (GM) and ground failure are represented by demand spectra curves. The building capacity curve is formed based on the generic EDP in the form of yield points (D_y, A_y) and ultimate points (D_u, A_u) by structure type, height, and level of code. The generic EDPs for building capacity curves are provided in the HAZUS manual. The capacity curve parameters used for this study are presented in Table 1, where the C1 structural type is for the low-rise category (1–3 floors) with variation in code level. The fragility curve for structural components is constructed using Equation 1, where the EDP used is the median value of spectral displacement at which the building reaches the threshold of the damage state ($\bar{S}_{d,ds}$) and the standard deviation of the natural logarithm of spectral displacement for the damage state (β_{ds}); there are four levels of damage: slight, moderate, extensive, and complete [7]. Each EDP for the damage level is provided in the HAZUS manual; the EDPs used for structural components in this study are illustrated in Table 1.

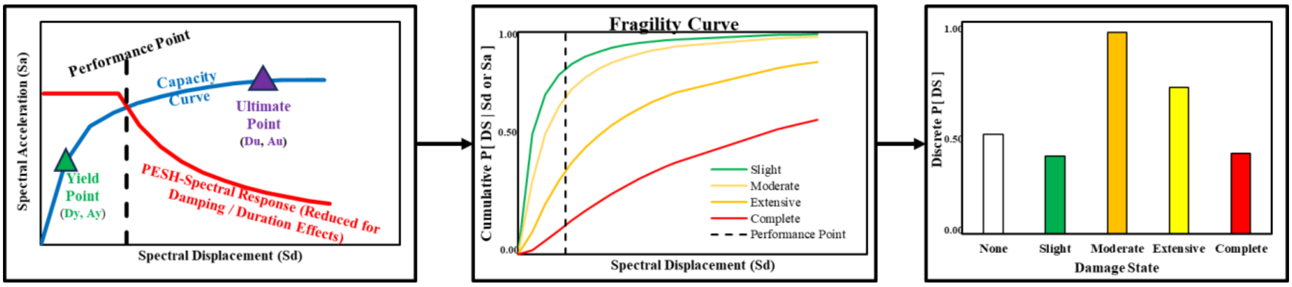

Fig. 1. Building Structural Damage Estimation Process in HAZUS [7].

Table 1. The empirical method capacity curve and fragility curve EDPs for concrete moment frame; low rise (C1L) [7] [32].

Method	Level of Building Code	Capacity Curve Parameter				Fragility Curve Parameter							
		Yield points		Ultimate Point		Slight		Moderate		Extensive		Complete	
		D_y (mm)	A_y (g)	D_u (mm)	A_u (g)	$\bar{S}_{d,ds}$ (mm)	β_{ds}	$\bar{S}_{d,ds}$ (mm)	β_{ds}	$\bar{S}_{d,ds}$ (mm)	β_{ds}	$\bar{S}_{d,ds}$ (mm)	β_{ds}
HAZUS Method	High-Code	9.93	0.25	238.43	0.75	22.86	0.81	45.72	0.84	137.16	0.86	365.76	0.80
	Moderate-Code	4.98	0.13	89.41	0.38	22.86	0.89	39.62	0.90	106.68	0.90	274.32	0.88
	Low-Code	2.49	0.06	37.26	0.19	22.86	0.95	36.58	0.91	91.44	0.85	228.60	0.97
RISK-EU Method	High-Code	0.70	0.13	5.90	0.26	6.30	0.65	13.20	0.75	20.10	0.85	47.80	0.95
	Moderate-Code	1.00	0.18	2.20	0.20	5.00	0.65	11.10	0.75	17.20	0.85	41.50	0.95
	Low-Code	6.40	0.05	29.00	0.08	2.00	0.65	4.10	0.75	6.20	0.85	14.70	0.95

$$P[ds \parallel S_d] = \Phi\left[\frac{1}{\beta_{ds}} \times ln\left(\frac{S_d}{\bar{S}_{d,ds}}\right)\right], \quad (1)$$

where the parameters are defined as follows:

S_d: Spectral displacement

$\bar{S}_{d,ds}$: Median value of spectral displacement at which the building reaches the threshold of the damage state, ds

β_{ds}: Standard deviation of the natural logarithm of spectral displacement for damage state, ds

Φ: Standard normal cumulative distribution function

The RISK-EU method is an empirical fragility curve method aimed at mapping vulnerability and estimating losses. It adopts many references from the HAZUS method, such as the hazard analysis method [32]. One of the distinguishing characteristics between the RISK-EU and HAZUS methods is the damage threshold factor. The damage threshold in the RISK-EU method is determined based on the capacity curve parameters, as shown in Figure 2, whereas in HAZUS, it is determined based on the building drift ratio limit.

The RISK-EU fragility curve model also has four levels of damage: slight, moderate, extensive, and complete. The yield point (A_y, D_y) and ultimate point (A_u, D_u) are built based on the available EDP, depending on the type of structure. The fragility curve is also built with the available EDP with damage limits from the results of the spectrum-based capacity analysis through Equation 1. The probability data for each damage level is used to calculate the replacement loss value of structural components. For this study, the capacity curve and fragility curve parameters used are depicted in Table 1.

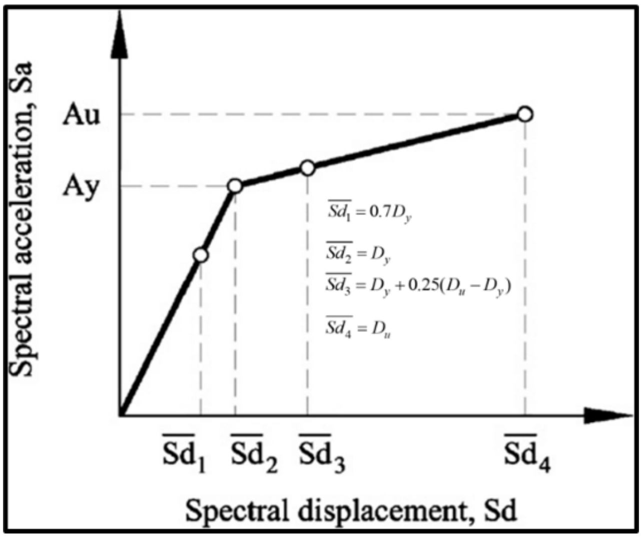

Fig. 2. The RISK-EU damage state thresholds [33].

2.2. Fragility curve development using the incremental dynamic analysis method

The IDA parametric analysis technique has recently surfaced in several forms to provide a more detailed estimate of structural performance under seismic loads [34]. It involves integrating one or more GM records, each scaled to numerous intensity levels, into a structural [34,35]. This produces one or more response curves, parameterized versus intensity level. Since the IDA method focuses on generating the fragility curve, the process of determining building performance uses the pushover method [36].

Before starting IDA, the structural model loaded by earthquake loads with selected GM data is analyzed to read the structural response in the form of story drift at each increase in earthquake load. In the first step, based on incremental load, a curve correlation between increased peak ground acceleration (PGA) and story drift is established.

The second step, developing the fragility curve through the IDA method, starts with the basic assumption that a structure's demand (D) is lognormally distributed, where the variable D is related to a normally distributed variable X by ln(D). The variable D is determined through Equation 2 [34]. The coefficients a and b in Equation 2 can be determined through regression analysis of the demand data derived through IDA or the proposed coefficient-based method through the logarithmic form in Equation 3 [37]. In this step, the correlation between PGA and story drift is defined as follows:

$$D = a(S_a)^b \quad (2)$$

$$X = ln(D) = ln(a) + b\, ln\,(IM) \quad (3)$$

where the parameters are defined as follows:

a, b: Coefficients of regression result of the IDA process

S_a: Spectral acceleration (g)

The variable PGA is used based on increased GM. This hazard parameter needs to be converted to spectral acceleration (S_a), the basis of hazard for the other empirical methods. In the third step, the conversion of PGA to S_a is conducted using the correlation between the height of the building, maximum story drift, drift factor, and the first natural period of the building [38]. The final target is the correlation between S_a and the spectral displacement. To obtain the EDP, the spectral displacement (S_d) is converted using the correlation between the height of the building, maximum story drift, and the drift factor [38].

In the fourth step, the coefficients *a* and *b* are determined using linear regression, still in logarithmic form [39]. From the correlation of S_a with S_d, the mean and standard deviation of X are determined through Equations 4 and 5 [37]. Based on the logarithmic form from these two parameters, the fragility curve function can be expressed in the form shown in Equation 6 [37]. The IDA probability equation has a form that is substantially different from Equation 1 used by the empirical method since Equation 1 is a simplified form of the IDA equation. Still, the probability calculation components have similarities in the parameters used. To define the fragility curve for each damage state, the story drift's damage threshold is set via the C variable:

$$m_x(Sa) = ln\,(a\,(Sa)^b) \tag{4}$$

$$\sigma_x = \sigma_{ln(D)} = \sqrt{\frac{1}{n-2}\sum_{i=1}^{n}\left[ln\left(\frac{\delta_i}{a(S_a)^b}\right)\right]^2} \tag{5}$$

$$P_f = P(D > C|S_a) = 1 - \Phi\left[\frac{ln(C) - m_x(S_a)}{\sigma_x}\right], \tag{6}$$

where the parameters are defined as follows:

P_f: Fragility curve function

C: Certain threshold or capacity on a given S_a

δ_i: Demand value

The probability value of the damage level obtained from each method (empirical and analytical) is used in determining the loss estimation discussed in Section 3.

3. Review of loss estimation analysis procedure

A review of previous fragility curve development methods shows significant differences regarding determining the extent of deterioration and the level of complexity. In determining building performance, the empirical method relies on the yield point and ultimate point EDPs in developing capacity curves that will be used in calculating building performance points; the EDPs are also compiled from a group of pushover analysis data used in the IDA method.

In the fragility curve development, determining the damage state limit is significant in all three methods. In the IDA and HAZUS methods, the damage state limits are calculated using the story drift parameter, although the limit value is different in both methods. For the RISK-EU method, the limit determination is considered based on the parameters on the capacity curve. The difference in the probability of damage levels generated by each method will vary from one another. Since all three methods have a final output on the probability of damage level, further reflection is needed to analyze the effect on loss estimation.

In this analysis, the formulation of the seismic loss value of the structure adopts the HAZUS method formula for the three methods presented in Equation 7. Here, the loss is calculated by accumulating the result of multiplying the probability value of each level of damage by the structural replacement ratio value to the building value for each level of damage; it is then multiplied by the building replacement cost (BRC), to obtain the damage loss value of the structural component. This study obtains BRCi from the national standard unit price for public buildings. The structural repair cost ratios for damage state ($RCS_{ds,i}$) are provided in the HAZUS manual for each damage state, where slight = 0.4%BRC, moderate = 1.9%BRC, extensive = 9.5%BRC, and complete = 18.9%BRC [7]. To assess the sensitivity of the probability values of each method to the estimated loss, the RCS parameter of HAZUS was held constant for all three methods.

$$CS_{ds,i} = BRC_i \times \sum_{i=1}^{33\Sigma} PMBTSTRds, i_{ds,i}, \tag{7}$$

where the parameters are defined as follows:

BRC_i: Building replacement cost

$PMBTSTR_{ds,i}$: Probability of structure being in structural damage state

$RCS_{ds,i}$: Structural repair cost ratio in damage state

The loss comparison is performed by calculating the average annual loss (AEL) estimate. The AEL simulation was conducted for each school building case study. In IDA (the analytical method), the EDP from the case study is used as the EDP representation for each level of code, whereas for HAZUS and RISK-EU (the empirical methods), the EDP for each technique is applied to the building database. The AEL is calculated based on eight hazard return periods (2,500, 2,000, 1,500, 1,000, 750, 500, 250, and 100 years) through Equation 8. It involves calculating the area in the average annual exceedance frequency plot against the estimated loss for each return period. In the Bandung city case study, the hazard parameters (S_{AS}, S_{A1}) available in the national earthquake source data are for the 2,500-year return period [40]. Equation 9 is used to obtain the hazard parameters for other return periods [41].

$$Annualized\ Losses = (P_{2500} \times L_{2500}) + \left[(P_{2000} - P_{2500}) \times \left(\frac{L_{2000}+L_{2500}}{2}\right)\right] + \left[(P_{1500} - P_{2000}) \times \left(\frac{L_{1500}+L_{2000}}{2}\right)\right] + \left[(P_{1000} - P_{1500}) \times \left(\frac{L_{1000}+L_{1500}}{2}\right)\right] + \left[(P_{750} - P_{1000}) \times \left(\frac{L_{750}+L_{1000}}{2}\right)\right] + \left[(P_{500} - P_{750}) \times \left(\frac{L_{500}+L_{750}}{2}\right)\right] + \left[(P_{250} - P_{500}) \times \left(\frac{L_{250}+L_{500}}{2}\right)\right] + \left[(P_{100} - P_{250}) \times \left(\frac{L_{100}+L_{250}}{2}\right)\right] \tag{8}$$

$$\frac{a_g}{a_{gR}} = \left(\frac{T}{T_R}\right)^2 \tag{9}$$

where the parameters are defined as follows:

L_i: Loss from each return period hazard

P_i: Average annual exceedance frequency (0.0004 for P_{2500}, 0.0005 for P_{2000}, 0.0007 for P_{1500}, 0.001for P_{1000}, 0.00133 for P_{750}, 0.002 for P_{500}, 0.004 for P_{250}, and 0.01 for P_{100})

a_g: Seismic acceleration value sought

a_{gR}: Reference value of earthquake acceleration

T: Return period value of the earthquake parameter being sought

T_R: Reference value of the return period of the known earthquake parameter

K: Seismic coefficient, taken as 0.3

Literature studies related to various methods of developing the fragility curve and determining the structural loss estimation from the plot results on the fragility curve are used as a reference method for this research; this will be explained more clearly in Section 4.

4. Methodology

This section will discuss the methodology used to achieve the objectives of this study based on the literature discussed in sections 2 and 3. The first step was to define the case studies. In this research, three school buildings were determined as case studies, representing each level of code determined based on the year the building was built, as shown in Table 2. The case studies are considered typical school buildings in Indonesia [42,43]. The level of code was determined based on the evolution of Indonesian seismic and concrete building codes [22]. The building data for schools selected as case studies is shown in Table 2. This shows that the floor height of the school building was typically 3–4 m. The building area of the schools was around 400 m^2. The data for earthquake acceleration parameters, S_{AS} and S_{A1}, were taken based on the 2017 Indonesia earthquake hazard source map, which follows the SNI 1726:2019 procedure for generating the standard spectral response; the site classification also utilizes the USGS 2016 Vs30 data [40,44,45]. The data show that all three case study buildings had a site class C.

Table 2. Data for school buildings in the case study.

Building Data		High Code Case Study	Moderate Code Case Study	Low Code Case Study
Year Built		2017	1998	1988
Number of Stories		3 (11.08 m)	2 (8.00 m)	2 (6.00 m)
Total Building Area (m^2)		410.48	409	496
Field Survey Data	f'_c (MPa)	18	18.2	21.9
Longitudinal Steel Reinf. Ratio (%)	Column	0.61–2.53	0.27–0.96	0.74–0.86
	Beam	0.33–1.77	0.73–1.45	0.58–1.27

In the second step, a field survey was conducted. Since no as-built drawing documentation existed, the survey was conducted to obtain building geometry data, structural component data, and existing concrete quality by the non-destructive test (NDT) method; rebar scanning was conducted to obtain existing concrete reinforcement data. The NDT tests on concrete were carried out using the rebound hammer and ultrasonic pulse velocity tests based on standard test methods [46,47]. The geometry survey was conducted using a laser meter. The results of the field survey are presented in Table 2. The quality of the concrete was at a moderate level of 18–21 MPa.

In the high-code case study (HC_{cs}), the building consisted of three floors, with a total height of 11.08 m, as shown in Figures 3a and 3b. The typical beam span between the main columns shown in Figure 3c was 4 m in the longitudinal direction and 7 m in the transverse direction. In the moderate-code case study (MC_{cs}), the building consisted of two floors, with a total height of 8.00 m, as shown in Figures 4a and 4b. The typical beam span between the main columns shown in Figure 4c was 3.2 m in the longitudinal direction and 6 m in the transverse direction. In the low-code case study (LC_{cs}), the building had two floors, with a total height of 6.00 m, as shown in Figures 5a and 5b. The typical beam span between the main columns shown in Figure 5c was 3.7 m in the longitudinal direction and 6.9 m in the transverse direction.

(a) Building photo

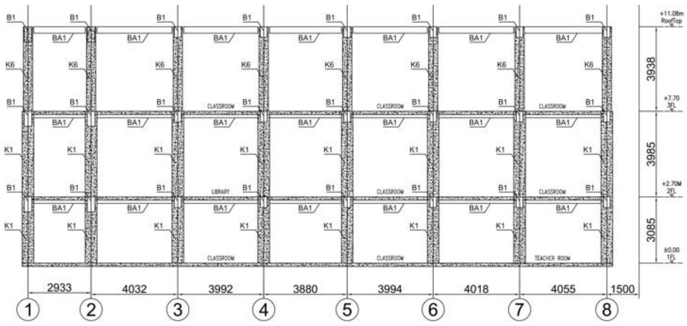

(b) Structure elevation view

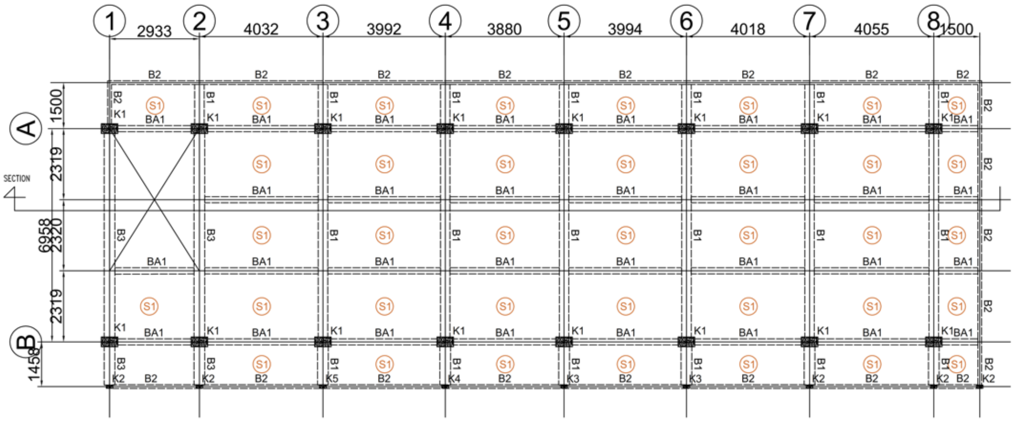

(c) Structure plan

Fig. 3. High-code school building case study.

(a) Building photo

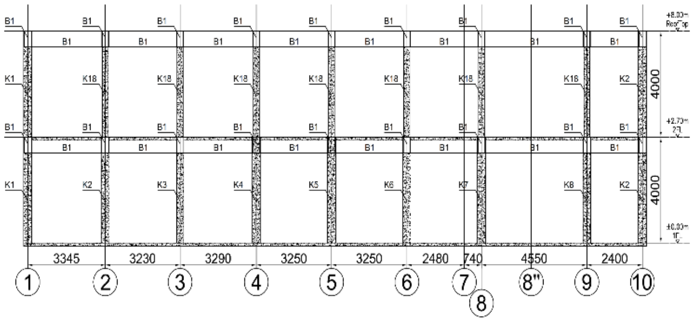

(b) Structure elevation view

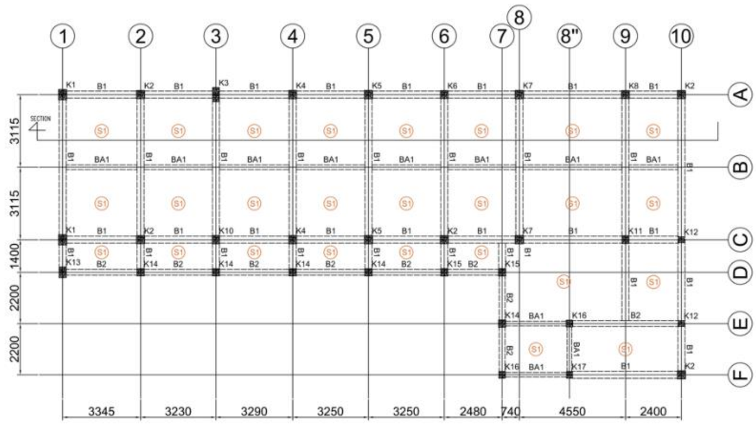

(c) Structure plan

Fig. 4. Moderate-code school building case study.

(a) Building photo

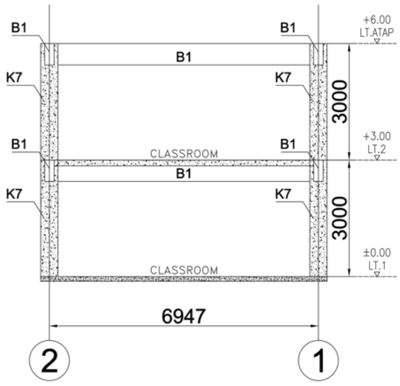

(b) Structure elevation view

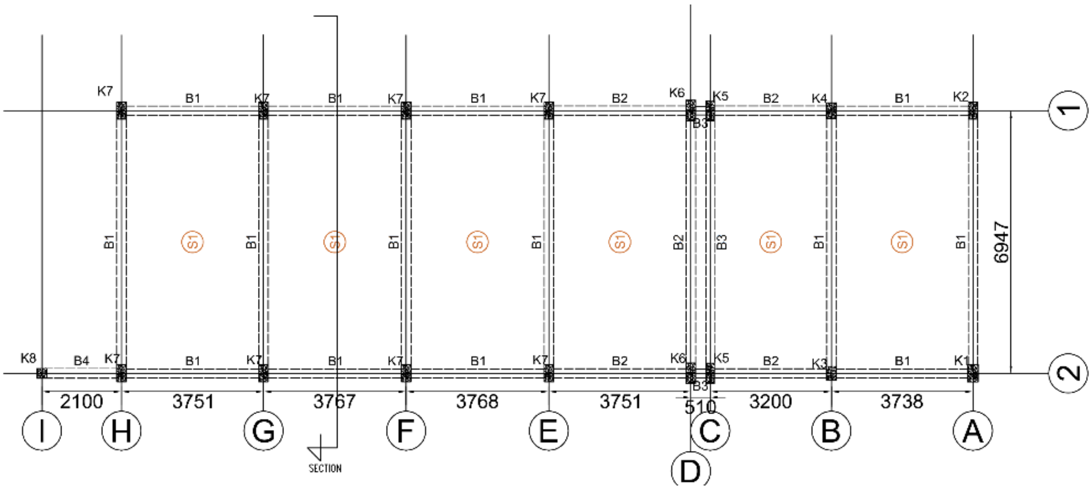

(c) Structure plan

Fig. 5. Low-code school building case study.

The comparison of column reinforcement for a typical main column for each level of code is shown in Figure 6. In the HC_{cs}, the longitudinal reinforcement ratio was 0.61%, which did not meet the 1%–6% requirement (SNI 2847:2013) of the local building high code. For the MC_{cs}, the longitudinal reinforcement ratio was 0.87%, which also did not meet the 1%–6% requirement (SNI 2847:2002) for the local building moderate code. In the LC_{cs}, the longitudinal reinforcement ratio was 1.03%, which fulfilled the 1%–6% local building low code requirement (PBI 1970).

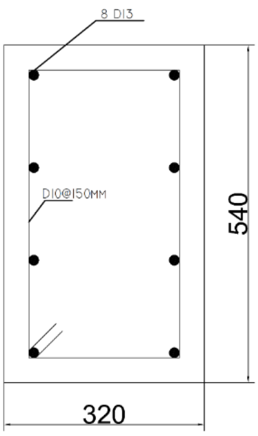

(a) High-code-K1

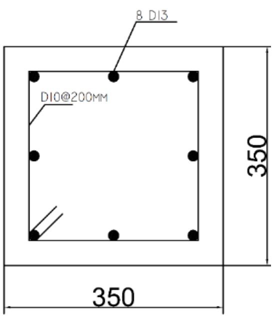

(b) Moderate-code-K2

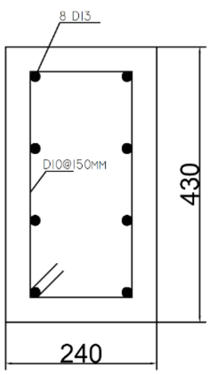

(c) Low-code-K7

Fig. 6. Column reinforcement.

The comparison of beam reinforcement for a typical primary beam in each level of code is shown in Figure 7. In the HC_{cs}, the longitudinal reinforcement ratio was 0.51%, which met the local building high code requirement (SNI 2847:2013) of 0.36%–2.5%. For the MC_{cs}, the longitudinal reinforcement ratio was 0.59%, which fulfilled the local building moderate code requirement (SNI 2847:2002) of 0.36%–2.5%. In the LC_{cs}, the longitudinal reinforcement ratio was 0.79%, which met the local building low code requirement (PBI 1970) of 0.36%–2.5%.

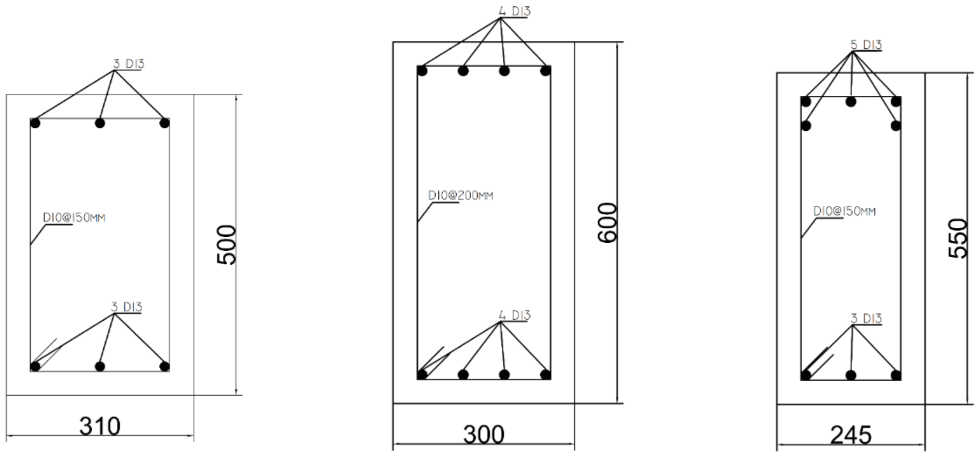

(a) High-code-B1 **(b)** Moderate-code-B1 **(c)** Low-code-B1

Fig. 7. Beam reinforcement.

Data from the survey results in the form of building property statistics (without a three-dimensional [3D] structural model) were used to develop capacity and fragility curves for the empirical methods (HAZUS and RISK-EU) based on the EDPs provided per the building classification. Based on the field survey data, the next step was 3D structural modeling in the ETABS software [48]. The pushover analysis was carried out from the 3D model of the structure, where the hinge property of the column and beam structure used modeling parameters based on the ASCE-41 standard [49]. The capacity curves generated from the empirical method and pushover analysis were compared to determine the performance point.

The 3D structural model was also used to construct the fragility curve using the IDA method. The GM data obtained from the Pacific Earthquake Engineering Research Center database was selected based on strike-slip and oblique mechanisms, with magnitudes of 5.6–7 Mw, which correspond to the parameters of strong earthquakes that have struck the Bandung City (the 2022 Cianjur and the 2009 Tasikmalaya earthquakes) [50–52]. The process of increasing the earthquake load was carried out with increments of 0.1 g following previous studies until the building response (story drift) reached/passed the damage threshold of the level of damage done. The damage threshold for the level of damage used for IDA in this study was adapted based on ATC and recommended by previous research on concrete frame low-rise buildings for drift ratio limits at the slight, moderate, extensive, and complete damage levels of 0.005, 0.010, 0.015, and 0.020, respectively [39]. The fragility curves obtained from the empirical and IDA methods were compared with the probability of each level of damage based on the performance points of each technique in the capacity curve comparison step. Based on the explanation of the study methodology above, the results to be discussed are the comparison of the capacity curve, fragility curve, and loss estimation obtained from the empirical and analytical methods.

5. Result and discussion

This section focuses on comparing EDPs from each method (capacity and fragility curves) and the loss estimates generated from the resulting EDPs.

5.1. Capacity curve comparative analysis

The capacity curve comparison analysis was performed by plotting the capacity curves from the three methods for each case study on one graph. In the pushover method, the capacity curve was raised in two directions, namely the longitudinal and transverse directions of the building. In determining the performance point, the maximum performance was determined at the intersection point with the hazard curve on both capacity curves. In the HAZUS method, the performance point is determined based on the intersection of the hazard curve with the median value, not on the deviation curve shown. The HAZUS deviation curves (+β and −β) are shown on the graph for comparison with the other two methods, where β is set as 0.25 for high code, moderate code, and low code [7]. The EDPs of pushover sequential yield points {Dy (mm), Ay (g)} and ultimate points (D_u (mm), A_u (g)} were {(39.51, 0.12); (147.84, 0.21)} for HC_{cs}, {(29.04, 0.21); (136.53, 0.33)} for MC_{cs}, and {(12.95, 0.25); (65.52, 0.41)} for LCcs.

A comparison of the capacity curves in the HC_{cs} is depicted in Figure 8a. The comparison indicates that the capacity curve from the HAZUS method is much larger than that of the RISK-EU and pushover methods. The capacity curves of the other two methods are also not yet in the HAZUS deviation range (−β). In contrast, the RISK-EU capacity curve is slightly closer to the case study pushover results in both directions. This indicates that the case study of the high code school building displays the same characteristics as the RISK-EU method.

The comparison of capacity curves in the MC_{cs} is presented in Figure 8b. The comparison highlights that the capacity curves of the three methods are in a relatively close range compared with the high code case study, although they show deviations. The RISK-EU method curve tends to be identical to the HAZUS method curve, as the curve is in the HAZUS deviation range (+β), while the pushover capacity curve is slightly below the HAZUS deviation limit (−β). The capacity curve indicates that the moderate code school building case study displays the same characteristics as the HAZUS and RISK-EU methods.

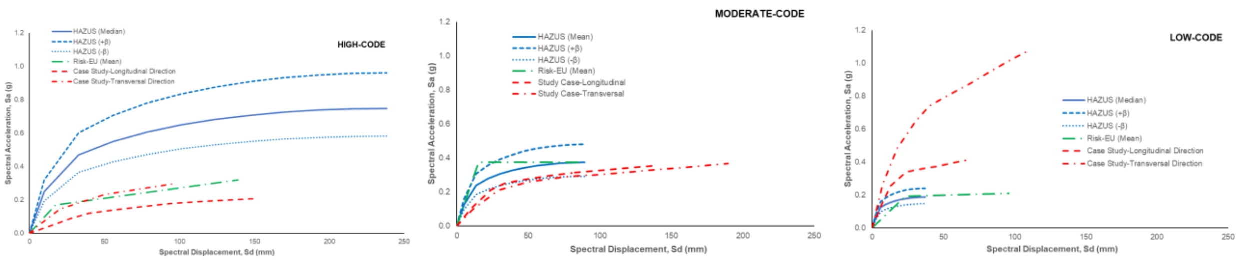

(a) HC_{cs} curves **(b)** MC_{cs} curves **(c)** LC_{cs} curves

Fig. 8. Capacity curve comparison.

A comparison of the capacity curves in the LC_{cs} is depicted in Figure 8c. The comparison shows that the capacity curve of the pushover results is relatively larger in both directions compared with the other two methods. The HAZUS and RISK-EU method curves tend to be identical, although the RISK-EU curve has a longer point estimate than the HAZUS curve. The capacity curves, therefore, indicate that the case study of low-code school buildings has a more significant similarity of characteristics with the HAZUS and RISK-EU methods. Based on a case study dependency, empirical EDPs can be employed by knowing the deviation used. In determining seismic loss, this comparative study concludes that the capacity curve still does not show a consistent trend. However, there are indications that empirical methods can be used, considering the pushover capacity curve in the β deviation range, as shown in two case studies (moderate and low codes). The variation of the deviation trend in the capacity curve shown in Figure 8 is in line with several previous case studies on the comparison of capacity curves in different case studies and regions [53,54]. Therefore, to assess the EDP capacity curve's sensitivity to loss estimation, a complete analysis of the overall EDP results, which are also influenced by the EDP fragility curve, is needed. The variation of the deviation is shown to affect the loss estimation in Section 5.3 in determining the building performance point, which is correlated with establishing the probability of damage level in the results of Section 5.2.

5.2. Fragility curve comparative analysis

The comparison analysis of fragility curves was conducted by plotting the third capacity curve of each method for each case study on one graph, as shown in Figures 9–11. According to Equation 6, the EDPs of IDA result sequential (a; b; and σ) were (1.00; 1.99; and 1.38) for HC_{cs}, (1.02; 1.75; and 1.56) for MC_{cs}, and (1.00; 2.18; and 2.86) for LC_{cs}. Meanwhile, the mean values varied according to the S_a values per Equation 4. The building performance obtained from the capacity curve analysis was used to determine the probability of damage levels in this analysis.

In the HC_{cs}, the order of building damage probability from highest to lowest for complete damage level was RISK-EU, IDA, and HAZUS, as shown in Figure 9d. The four damage levels show a trend where the RISK-EU method results are consistently the most fragile; the IDA method shows a gradual shift from the slight damage level to the complete damage level, where it ranks between RISK-EU and HAZUS for fragility, as shown in Figures 9a–d. In the MC_{cs}, the order of building damage probability from highest to lowest for complete damage level was RISK-EU, IDA, and HAZUS, as shown in Figure 10d. The MC_{cs} shows the same trend in the IDA method as the high code case study, as shown in Figures 10a–d. In the LC_{cs}, the order of building damage probability from highest to lowest for complete damage level was RISK-EU, IDA, and HAZUS, as shown in Figure 11d. The LC_{cs} also shows the same trend in the IDA method as the HC_{cs}, as shown in Figures 11a–d. The RISK-EU method results consistently became the most fragile compared with the other two methods.

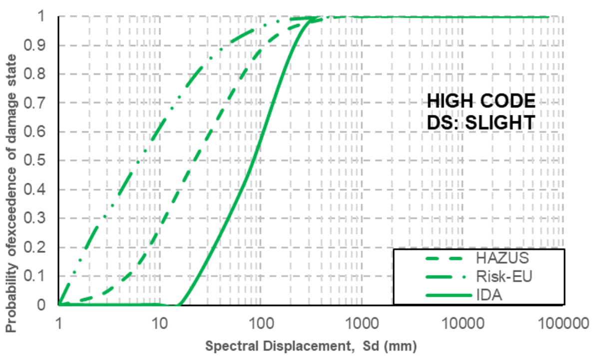

(a) Slight damage.

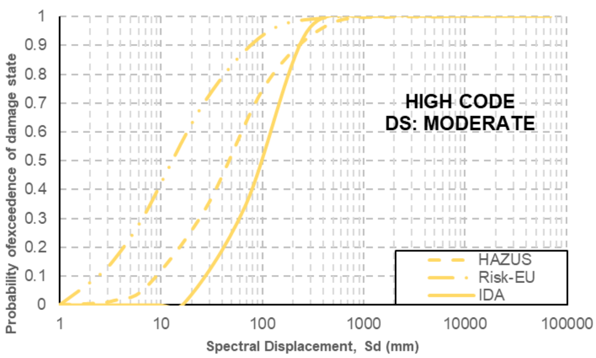

(b) Moderate damage.

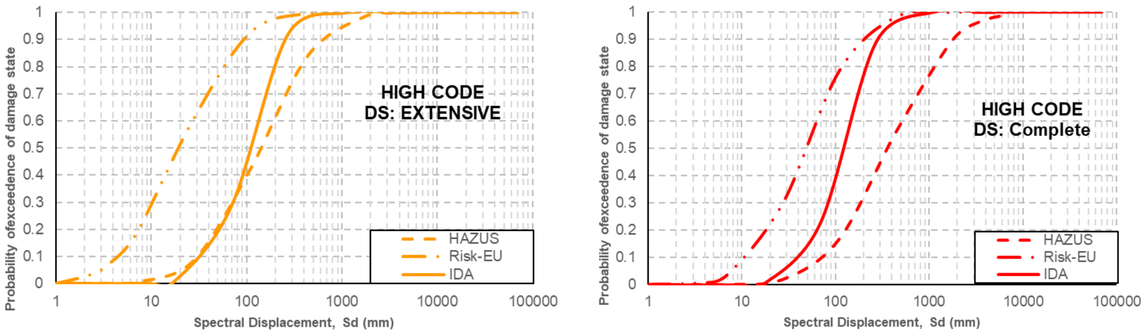

(c) Extensive damage **(d)** Complete damage

Fig. 9. HCcs fragility curve comparison in various damage states.

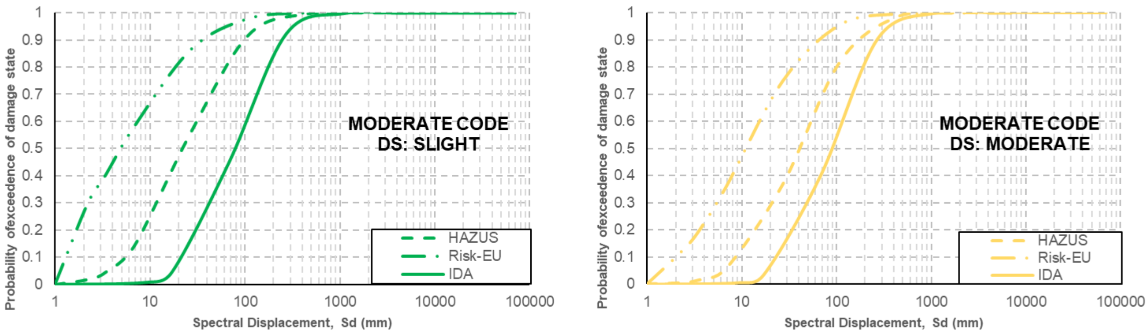

(a) Slight damage **(b)** Moderate damage

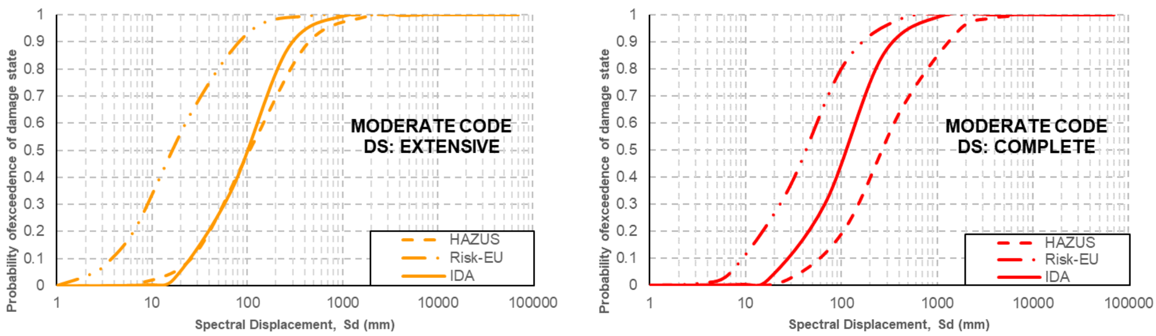

(c) Extensive damage **(d)** Complete damage

Fig. 10. MC_{cs} fragility curve comparison in various damage states.

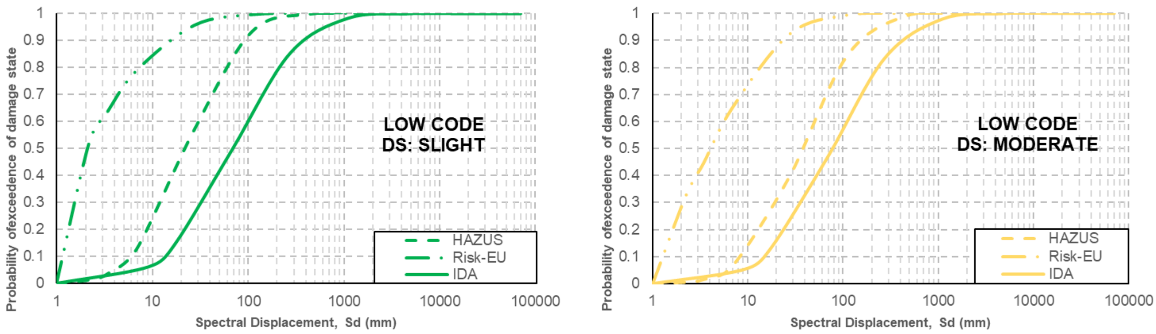

(a) Slight damage **(b)** Moderate damage

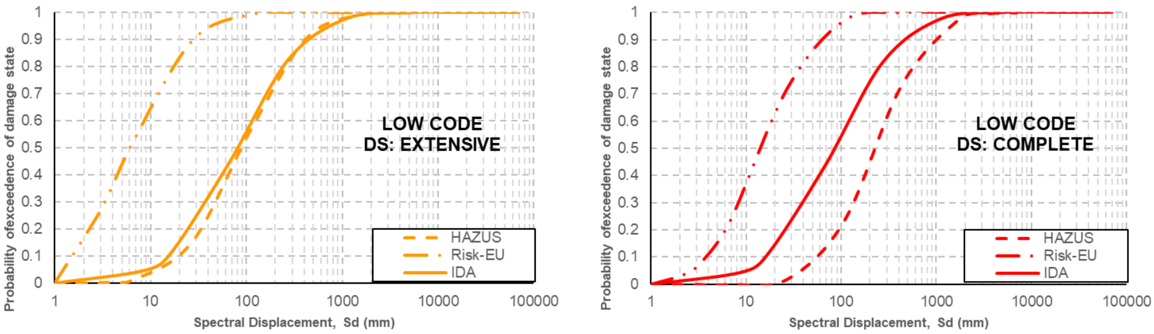

(c) Extensive damage **(d)** Complete damage

Fig. 11. LCcs fragility curve comparison in various damage states.

The differences in damage thresholds also explain the consistent trend of shifting the fragility curve position of the IDA method in all three case studies, where the damage threshold has been presented in each method. The comparison was made based on the same damage threshold, namely story drift, in the HAZUS and IDA methods. Taking the case of low code as an example, the damage limits in the HAZUS method results for slight, moderate, extensive, and complete damage levels are 0.005, 0.008, 0.020, and 0.050, respectively; in IDA results, these limits are 0.005, 0.010, 0.015, and 0.020, respectively [7,39]. At the slight damage level, both have the same damage limit (0.005). In moderate damage, there is a difference; however, it is still relatively small (0.010 – 0.008 = 0.002). In extensive damage, the HAZUS method has the same limit as the complete IDA damage level limit of 0.02; this shows that there is a shift that coincides between the HAZUS and IDA methods results. On the complete damage level, the HAZUS method fragility curve is already between the RISK-EU and HAZUS curves, where the damage limit is wider (0.05) than IDA (0.020). The same is true for the other two case studies. The trend of the case study curve being more "fragile" than the standard HAZUS fragility curve at varying levels of damage in this study is consistent with the indications of the study results in several building case studies in different regions outside the US [55–58]. The comparison of the fragility curve between the empirical and analytical methods above shows a deviation. The variation of the deviation will be seen to influence the loss estimation in Section 5.3 in determining the probability of building damage.

5.3. Seismic loss comparative analysis

The comparative analysis of estimated earthquake loss was calculated based on eight hazard return periods (2,500, 2,000, 1,500, 1,000, 750, 500, 250, and 100 years) per the national hazard map. A comparison of the loss estimation values was performed in %BRC unit values to assess the sensitivity of the influence on the EDPs of the three methods. The significance of EDP's effect on loss is measured based on the resulting estimated value, which is considerably effective based on the sensitivity analysis of the hazard parameters to the loss estimates of previous studies [59]. The results of the estimation of each method and return period are shown in Figure 12 and Table 3 for a complete recap of the loss estimates for each return period. In the high code case, the estimated loss calculated using the IDA method is close to the RISK-EU method at large return periods but gradually approaches the HAZUS method results for small return periods, as shown in Figure 12a. The difference between the IDA method and HAZUS results at return periods of 2500, 500, and 100 years for the high code case are 11.85%BRC, 5.07%BRC, and 1.01%BRC, respectively, while the deviation range of the IDA method against RISK-EU at return periods of 2500, 500, and 100 years are 0.61%BRC, 6.48%BRC, and 0.3%BRC as shown in Figure 12a. Regarding the AEL difference with the IDA method in each high-code case study, HAZUS has a deviation of 0.03%BRC, and RISK-EU has a deviation of 0.05%BRC, as shown in Figure 13.

In the case of moderate code, the estimated loss calculated using the IDA method was close to HAZUS method results, entirely from large to small return periods, as shown in Figure 12b. The difference between the IDA and HAZUS method results at return periods of 2500, 500, and 100 years for the moderate code case study is 3.75%BRC, 1.17%BRC, and 0.13%BRC, respectively, while the deviation range of the IDA method against RISK-EU at return periods of 2500, 500, and 100 years is 5.23%BRC, 10.86%BRC, and 7.29%BRC as shown in Figure 12b. Regarding the AEL difference with the IDA method in each high-code case study, HAZUS has a deviation of 0.01%BRC, and RISK-EU has a deviation of 0.11%BRC, as shown in Figure 13.

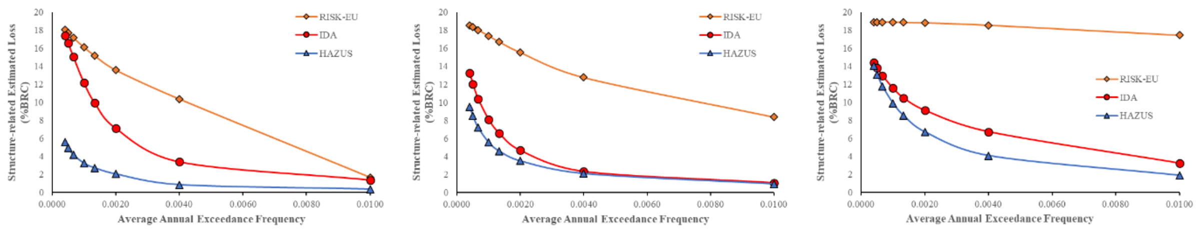

(a) HC_{cs} **(b)** MC_{cs} **(c)** LC_{cs}

Fig. 12. Estimated losses comparison in each return period hazard scenario.

Table 3. Estimated losses comparison on each return period hazard scenario.

Case	Estimated Loss (%BRC)	Return Period (Average Annual Exceedance Frequency)							
		2500 (0.0004)	2000 (0.0005)	1500 (0.0007)	1000 (0.0010)	750 (0.0013)	500 (0.0020)	250 (0.0040)	100 (0.0100)
High Code	RISK-EU	18.05	17.72	17.18	16.14	15.20	13.59	10.38	1.67
	IDA	17.44	16.61	15.08	12.18	9.97	7.12	3.39	1.38
	HAZUS	5.60	4.95	4.18	3.25	2.73	2.05	0.86	0.37
Moderate Code	RISK-EU	18.51	18.34	18.03	17.37	16.71	15.53	12.76	8.37
	IDA	13.28	12.04	10.39	8.09	6.57	4.67	2.35	1.08
	HAZUS	9.53	8.49	7.20	5.56	4.59	3.50	2.11	0.95
Low Code	RISK-EU	18.90	18.90	18.89	18.88	18.86	18.81	18.55	17.47
	IDA	14.45	13.84	12.96	11.57	10.49	9.12	6.74	3.25
	HAZUS	14.07	13.10	11.78	9.89	8.52	6.72	4.10	1.91

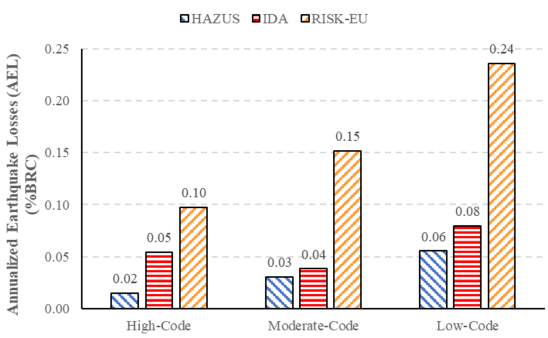

Fig. 13. Structure-related AEL data comparison.

In the case of low code, the estimated loss calculated using the IDA method was also close to HAZUS results, completely from large to small return periods, as shown in Figure 12c. The difference between the IDA and HAZUS methods results at return periods of 2500, 500, and 100 years for the low-code case studies are 0.38%BRC, 2.40%BRC, and 1.35%BRC, respectively; the deviation range of the IDA method results against RISK-EU method results at return periods of 2500, 500, and 100 years are 4.45%BRC, 9.69%BRC, and 14.21%BRC as shown in Figure 12c. Regarding the AEL difference with the IDA method in each high-code case study, HAZUS has a deviation of 0.02%BRC, and RISK-EU has a deviation of 0.16%BRC, as shown in Figure 13.

The comparison of relative deviation between empirical and analytical methods is shown in Table 4. Since the empirical model is a pre-disaster model and does not have actual loss data, the analytical calculation is used as a reference to measure the sensitivity level because it uses a detailed and rigorous method. Table 4 shows that the difference in EDP has significance on loss estimation in line with the significance of EDP deviation comparison of the capacity and fragility curves. In high code, the average relative deviation of HAZUS to the analytical method is 71.90% in single hazard scenario and a deviation of 72.18% in AEL; in contrast, the average relative deviation of RISK-EU to the analytical method is 53.44% in single hazard scenario, and a deviation of 79.78% in AEL, as shown in Table 4. In moderate code, the average relative deviation of HAZUS to the analytical method is 24.66% in a single hazard scenario. The deviation is 21.16% in AEL, while the average relative deviation of RISK-EU to the analytical method is 222.82% in a single hazard scenario. The deviation is 295.49% in AEL, shown in Table 4. At low code, the average relative deviation of HAZUS to the analytical method is 19.66% in the single hazard scenario and a deviation of 30.23% in the AEL. In comparison, the average relative deviation of RISK-EU to the analytical method is 121.79% in the single hazard scenario and a deviation of 196.87% in the AEL, shown in Table 4.

Table 4. Relative difference in estimated loss comparison.

Case	Relative Difference	Return Period (Average Annual Exceedance Frequency)								AEL
		2500 (0.0004)	2000 (0.0005)	1500 (0.0007)	1000 (0.0010)	750 (0.0013)	500 (0.0020)	250 (0.0040)	100 (0.0100)	
High Code	│IDA - HAZUS│ / IDA	67.91%	70.18%	72.29%	73.35%	72.63%	71.18%	74.62%	73.03%	72.18%
	│IDA - RISK-EU│/ IDA	3.48%	6.67%	13.93%	32.49%	52.41%	91.01%	206.07%	21.45%	79.78%
Moderate Code	│IDA - HAZUS│ / IDA	28.25%	29.48%	30.72%	31.33%	30.19%	25.04%	10.18%	12.12%	21.16%
	│IDA - RISK-EU│/ IDA	39.38%	52.33%	73.56%	114.70%	154.19%	232.61%	443.72%	672.03%	295.49 %
Low Code	│IDA - HAZUS│ / IDA	2.61%	5.37%	9.11%	14.50%	18.72%	26.28%	39.27%	41.44%	30.23%
	│IDA - RISK-EU│/ IDA	30.81%	36.55%	45.75%	63.19%	79.84%	106.21%	175.04%	436.91%	196.87 %

The relative comparison above shows that EDP has a significant influence on the loss estimation in the single hazard scenario as well as in the AEL. However, from Table 3, it can be calculated that the absolute deviation value of the loss estimate from the analytical model is <12%BRC (range 0.13%–11.85%RBC) for the HAZUS model and <15%BRC (range 0.30%–14.21%RBC) for the RISK-EU model in the single hazard scenario. The significance of EDP in this study indicates the significance of characterizing building EDP in local buildings for loss estimation. However, as stated earlier, the findings of absolute deviation values can be a consequential reference when adopting empirical models for structural loss estimation, considering the adoption process as a tactical solution in accelerating and expanding loss estimation in line with the UN's (SDGs) program for developing countries, in addition to the parallel strategy of mapping EDP characteristics, which requires a lot of time and resources. The absolute deviation of <12%–15%BRC addresses the gap left by previous studies that directly adopted EDP from empirical models (HAZUS and RISK-EU) [60–66]. The absolute deviation reference is reliable in the method adoption process considering that this case study represents the level of code and various hazard and AEL scenarios. In the context of adoption in Indonesia, the HAZUS method has the potential for adoption with minimum deviation, both in terms of estimation value and relative deviation. Of course, the deviation is also adjusted to the risk profile of the authority in the budgeting process related to the disaster. This deviation value can be used as an adjustment coefficient for budgeting, especially since the HAZUS method provides conceptual-level estimates before disasters occur. Yet, it remains reliable for long-term disaster relief needs.

This EDP needs to be further developed based on local building characteristics for more detailed identification of damage probabilities. The process can begin with the typical buildings that most represent the population buildings, as seen in this study and previous studies [31]. This study provides an overview of the data on how large the deviation is when adopting an existing loss estimation tool. Previous studies have shown the confidence of direct adoption, ignoring the subsequent differences. Although, in the end, this study showed favorable results toward adoption, an overview of the deviation value as a consequence of method adoption was obtained.

6. Conclusion

This study compares empirical and analytical EDP methods on capacity and fragility curves and their influence on estimating structural component loss. The comparison of capacity curves shows that there is a variation where the capacity of the empirical method is greater for the case study building for the high-code and moderate-code cases, while the reverse occurs in the low-code cases, as shown in Figure 8. The comparison of fragility curves shows that the fragility curve obtained using the analytical method, at the complete damage level, is consistently more “fragile” than the one obtained using the empirical HAZUS method but not more “fragile” than the RISK-EU method one.

EDP has a significant effect on structural component loss estimation, based on the deviation relative to the analytical method, with a deviation range of (2.61%–672.03%) for both empirical methods. However, another study finding is that the absolute deviation value against the analytical method shows a deviation range of <12%–15%BRC. The absolute deviation value could be a critical finding of the consequences of directly adopting EDP from the empirical method shown in the previous study. In addition, this absolute deviation can also be a short-term solution for decision-makers in developing countries that do not yet have an EDP database to consider in the process of adopting and estimating earthquake losses in their region.

This study is limited to the effect of EDP on loss estimation of structural components. Future research can explore the effect of EDP on nonstructural components. In addition, future studies can also focus on the effect of variable sensitivity of reconstruction costs on loss estimation. Through the findings of this study, it can be considered to adopt empirical methods as a short-term solution to strengthen financial resilience to earthquakes.

Funding

This work was supported by the Higher Education Financing Centre (BPPT) Ministry of Education, Culture, Research, and Technology of the Republic of Indonesia and Indonesia Endowment Fund for Education (LPDP), Ministry of Finance Republic of Indonesia under Grant [202101122157].

The author would also like to thank Institut Teknologi Bandung, The Bandung City Education Office, and the schools involved in this study for providing facilities during research activities.

Conflicts of interest

The authors declare that they have no known competing financial interests or personal relationships that could have appeared to influence the work reported in this paper.

Authors contribution statement

Roi Milyardi: Formal analysis; Roles/Writing – original draft; Data curation.

Krishna Suryanto Pribadi: Conceptualization; Supervision.

Muhamad Abduh: Supervision; Writing – review & editing.

Irwan Meilano: Writing – review & editing; Visualization.

Erwin Lim: Data curation; Methodology; Investigation.

Reini Djuhraeni Wirahadikusumah: Resources; Supervision.

Patria Kusumaningrum: Validation; Software.

Eliza Rosmaya Puri: Project administration; Supervision.

References

[1] Navas-Sánchez L, Jiménez-Martínez M, González-Rodrigo B, Hernández-Rubio O, Dávila-Migoya LD, Orta-Rial B, et al. A methodology to assess and select seismic fragility curves: Application to the case of Costa Rica. Earthq Spectra 2023;39:1380–409.

[2] Adibi M, Talebkhah R. Seismic Reliability of the Non-Code-Conforming RC Building Due to Vertical Mass Irregularity Effect. J Rehabil Civ Eng 2022;10:14–32. https://doi.org/10.22075/JRCE.2021.23630.1516.

[3] Irfan Z, Abdullah, Afifuddin M. Development of fragility curve based on incremental dynamic analysis curve using ground motion Aceh earthquake. E3S Web Conf 2022.

[4] Bose S, Stavridis A, Anastasopoulos P, Sett K. Fragility Curves For A School Building In Nepal Accounting For Uncertainties In Material Parameters. 18th World Conf. Earthq. Eng., 2024, p. 1–12.

[5] Seki M, Nakajima Y, Matsuo J, Marukawa R. Application Of Simplified Seismic Evaluation Methods For Existing RC Buildings in Myanmar. 18th World Conf. Earthq. Eng., 2024, p. 1–12. https://doi.org/https://doi.org/10.1007/s10518-021-01083-3.

[6] Milyardi R, Pribadi KS, Meilano I, Lim E. Identifying the potential development of HAZUS model as an earthquake disaster loss model for school buildings in Indonesia. IOP Conf Ser Earth Environ Sci 2023;1244. https://doi.org/10.1088/1755-1315/1244/1/012022.

[7] FEMA-NIBS. HAZUS Earthquake Model Technical Manual. Fed Emerg Manag Agency 2020.

[8] Crowley H, Despotaki V, Silva V, Dabbeek J, Romão X, Pereira N, et al. Model of seismic design lateral force levels for the existing reinforced concrete European building stock. Bull Earthq Eng 2021;19:2839–65. https://doi.org/https://doi.org/10.1007/s10518-021-01083-3.

[9] Solanki VR, Jadhav P, Prashant A. Uncertainties of shear forces and bending moments in retaining wall due to earthquake loading. Adv. Comput. Methods Geomech. IACMAG Symp. 2019 Vol. 1, Springer; 2020, p. 39–47. https://doi.org/10.1007/978-981-15-0886-8_4.

[10] Ansari A, Seshagiri Rao K, Jain AK. Seismic Microzonation of the Himalayan Region Considering Site Characterization: Application toward Seismic Risk Assessment for Sustainable Tunneling Projects. Nat Hazards Rev 2024;25. https://doi.org/10.1061/nhrefo.nheng-1815.

[11] Thadagani KS, Ansari A, Seshagiri Rao K, Shekhar S. Investigating the response of Urban Underground Utilities (3U) within an elastic and elastoplastic geological formation: Employing numerical and analytical techniques. Model Earth Syst Environ 2024;10:4921–37. https://doi.org/10.1007/s40808-024-02042-y.

[12] Hancilar U, Sesetyan K, Cakti E. Comparative earthquake loss estimations for high-code buildings in Istanbul. Soil Dyn Earthq Eng 2020;129:105956. https://doi.org/10.1016/j.soildyn.2019.105956.

[13] Lee J-H, Ansari A, An H, Jeong J-Y. Seismic loss and resilience modeling of bridges in soft soils: towards the design of sustainable transportation infrastructure facilities. Sustain Resilient Infrastruct 2024;9:473–95. https://doi.org/10.1080/23789689.2024.2328979.

[14] Ansari A, Rao KS, Jain AK. An integrated approach to model seismic loss for the Himalayan infrastructure projects: Decision-making and functionality concept for disaster mitigation. Bull Eng Geol Environ 2023;82:1–12. https://doi.org/10.1007/s10064-023-03422-x.

[15] BPS. Total Population by Regency/City in West Java, 2018-2020 2020. https://jabar.bps.go.id/indicator/12/133/1/jumlah-penduduk-menurut-kabupaten-kota.html (accessed September 14, 2022).

[16] Sari AM, Fakhrurrozi A, Syahbana AJ, Sarah D, Setiadi B, Daryono MR, et al. Seismic hazard on West Bandung district using non-linear earthquake response analysis. E3S Web Conf 2021;331:07003. https://doi.org/10.1051/e3sconf/202133107003.

[17] Handayani AP, Prasetyaningrum AA, Klicek T, Aswin R. Building Resilience through Sustainable Tourism: A Case Study of Lembang and Greater Bandung Area 2023. https://doi.org/http://doi.org/10.37502/IJSMR.2023.61103.

[18] Daryono MR, Natawidjaja DH, Sapiie B, Cummins P. Earthquake Geology of the Lembang Fault, West Java, Indonesia. Tectonophysics 2019;751:180–91. https://doi.org/10.1016/j.tecto.2018.12.014.

[19] BNPB. Data Informasi Bencana Indonesia 2022. https://dibi.bnpb.go.id/xdibi (accessed May 24, 2022).

[20] BPS. Indonesia's Education Statistics 2020. Jakarta: Badan Pusat Statistik; 2020.

[21] Milyardi R, Desiani A, Wong H, Setiawan D, Husada G. Assessment of Seismic Vulnerability of School Buildings: A case study in Bandung, West Java, Indonesia. Disaster Adv 2023;16:49–59. https://doi.org/10.25303/1609da049059.

[22] Nugroho WO, Sagara A, Imran I. The evolution of Indonesian seismic and concrete building codes: From the past to the present. Structures 2022;41:1092–108. https://doi.org/10.1016/j.istruc.2022.05.032.

[23] Muntafi Y, Nojima N, Jamal AU. Damage Probability Assessment of Hospital Buildings in Yogyakarta, Indonesia as Essential Facility due to an Earthquake Scenario. J Civ Eng Forum 2020;6:225. https://doi.org/10.22146/jcef.53387.

[24] Aulady MFN, Fujimi T. Earthquake loss estimation of residential buildings in bantul regency, Indonesia. Jamba J Disaster Risk Stud 2019;11:1–10. https://doi.org/10.4102/jamba.v11i1.756.

[25] Alam MS, Haque SM. Multi-dimensional earthquake vulnerability assessment of residential neighborhoods of Mymensingh City, Bangladesh: A spatial multi-criteria analysis based approach. J Urban Manag 2022;11:37–58. https://doi.org/10.1016/j.jum.2021.09.001.

[26] Jamal-ud-din, Ainuddin S, Murtaza G, Faiz S, Muhammad AS, Raheem A, et al. Earthquake vulnerability assessment through spatial multi-criteria analysis: a case study of Quetta city, Pakistan. Environ Earth Sci 2023;82:1–19. https://doi.org/10.1007/s12665-023-10967-3.

[27] Saretta Y, Sbrogio L, Valluzzi MR. Seismic response of masonry buildings in historical centres struck by the 2016 Central Italy earthquake. Calibration of a vulnerability model for strengthened conditions. Constr Build Mater 2021;299:123911. https://doi.org/https://doi.org/10.1016/j.conbuildmat.2021.123911.

[28] Freddi F, Galasso C, Cremen G, Dall'Asta A, Di Sarno L, Giaralis A, et al. Innovations in earthquake risk reduction for resilience: Recent advances and challenges. Int J Disaster Risk Reduct 2021;60:102267. https://doi.org/https://doi.org/10.1016/j.ijdrr.2021.102267.

[29] Gandage S, Goel MD. Seismic Fragility Assessment of RC Building Using HAZUS Methodology and Incremental Dynamic Analysis. ASPS Conf Proc 2022;1:731–8. https://doi.org/10.38208/acp.v1.575.

[30] Felsenstein D, Elbaum E, Levi T, Calvo R. Post-processing HAZUS earthquake damage and loss assessments for individual buildings. Nat Hazards 2021;105:21–45. https://doi.org/10.1007/s11069-020-04293-1.

[31] Aroquipa H, Hurtado AI. Incremental seismic retrofitting for essential facilities using performance objectives: A case study of the 780-PRE school buildings in Peru. J Build Eng 2022;62:105387. https://doi.org/10.1016/j.jobe.2022.105387.
[32] Milutinovic Z V., Trendafiloski GS. WP4 Vulnerability of Current Buildings. 2003.
[33] Cardona OD, Ordaz MG, Yamin LE, Marulanda MC, Barbat AH. Earthquake loss assessment for integrated disaster risk management. J Earthq Eng 2008;12:48–59. https://doi.org/10.1080/13632460802013495.
[34] Vamvatsikos D, Allin Cornell C. Incremental dynamic analysis. Earthq Eng Struct Dyn 2002;31:491–514. https://doi.org/10.1002/eqe.141.
[35] Vamvatsikos D, Cornell CA. Application of Incremental Dynamic Analysis to an RC- Structure 1966:1–12.
[36] Vamvatsikos D, Cornell CA. The Incremental Dynamic Analysis and Its Application To Performance-Based Earthquake Engineering. 12th Eur. Conf. Earthq. Eng., 2002, p. 10.
[37] Samadian D, Ghafory-Ashtiany M, Naderpour H, Eghbali M. Seismic resilience evaluation based on vulnerability curves for existing and retrofitted typical RC school buildings. Soil Dyn Earthq Eng 2019;127:105844. https://doi.org/10.1016/j.soildyn.2019.105844.
[38] K.L. Su R. Typical Collapse Modes of Confined Masonry Buildings under Strong Earthquake Loads. Open Constr Build Technol J 2011;5:50–60. https://doi.org/10.2174/1874836801105010050.
[39] Su RKL, Lee CL. Development of seismic fragility curves for low-rise masonry infilled reinforced concrete buildings by a coefficient-based method. Earthq Eng Eng Vib 2013;12:319–32. https://doi.org/10.1007/s11803-013-0174-0.
[40] PUSGEN. Indonesia Earthquake source and hazard map 2017. Bandung: Ministry of Public Works and Housing of Indonesia; 2017.
[41] CEN. Eurocode 8 - Design of structures for earthquake resistance Part 2: Bridges. 2005.
[42] Idris Y, Cummins P, Rusydy I, Muksin U, Syamsidik, Habibie MY, et al. Post-Earthquake Damage Assessment after the 6.5 Mw Earthquake on December, 7th 2016 in Pidie Jaya, Indonesia. J Earthq Eng 2022;26:409–26. https://doi.org/10.1080/13632469.2019.1689868.
[43] Gentile R, Galasso C, Idris Y, Rusydy I, Meilianda E. From rapid visual survey to multi-hazard risk prioritisation and numerical fragility of school buildings. Nat Hazards Earth Syst Sci 2019;19:1365–86. https://doi.org/10.5194/nhess-19-1365-2019.
[44] USGS, arcgis. Vs30 Map Viewer 2023. https://usgs.maps.arcgis.com/apps/webappviewer/index.html?id=8ac19bc334f747e486550f32837578e1 (accessed September 15, 2022).
[45] BSN. SNI 1726-2019 - Procedures for Planning Earthquake Resistance for Building and Non-Building Structures. Jakarta: Badan Standardisasi Nasional; 2019.
[46] BSN. Test method for wave propagation speed through concrete (SNI ASTM C597:2012). 2012.
[47] BSN. Hard concrete reflective number test method (ASTM C 805-02 , IDT)-SNI ASTM C597 : 2012. Jakarta: Badan Standarisasi Nasional; 2012.
[48] Computers and Structures Inc. ETABS Training manuals 2023. https://wiki.csiamerica.com/display/doc/ETABS+Training+manuals (accessed November 26, 2023).
[49] ASCE/SEI. Asce/SEI 41-17. 2017.
[50] PEER. PEER Ground Motion Database 2023. https://ngawest2.berkeley.edu/ (accessed November 26, 2023).
[51] Supendi P, Winder T, Rawlinson N, Bacon CA, Palgunadi KH, Simanjuntak A, et al. A conjugate fault revealed by the destructive Mw 5.6 (November 21, 2022) Cianjur earthquake, West Java, Indonesia. J Asian Earth Sci 2023;257:105830. https://doi.org/https://doi.org/10.1016/j.jseaes.2023.105830.
[52] Gunawan E, Widiyantoro S, Marliyani GI, Sunarti E, Ida R, Gusman AR. Fault source of the 2 September 2009 Mw 6.8 Tasikmalaya intraslab earthquake, Indonesia: Analysis from GPS data inversion, tsunami height simulation, and stress transfer. Phys Earth Planet Inter 2019;291:54–61. https://doi.org/https://doi.org/10.1016/j.pepi.2019.04.004.
[53] Muntafi Y. Development of Pushover Analysis on HAZUS Method to Determine Building Damage Probability as an Earthquake Mitigation Efforts 2016.
[54] Lang DH, Singh Y, Prasad JSR. Comparing empirical and analytical estimates of earthquake loss assessment studies for the city of Dehradun, India. Earthq Spectra 2012;28:595–619. https://doi.org/10.1193/1.4000004.

[55] Baker JW. Measuring bias in structural response caused by ground motion scaling. Pacific Conf Earthq Eng 2007:1–6. https://doi.org/10.1002/eqe.

[56] Bermúdez CA, Barbat AH, Pujades L. Seismic vulnerability and fragility of steel buildings. World Conf Earthq Eng 2008:1–8.

[57] Uma SR, Ryu H, Luco N, Liel AB, Raghunandan M. Comparison of main-shock and aftershock fragility curves developed for New Zealand and US buildings. 9th Pacific Conf Earthq Eng 2011:1–9.

[58] Mansouri I, Hu JW, Shakeri K, Shahbazi S, Nouri B. Assessment of Seismic Vulnerability of Steel and RC Moment Buildings Using HAZUS and Statistical Methodologies. Discret Dyn Nat Soc 2017;2017. https://doi.org/10.1155/2017/2698932.

[59] Andrade RB, Pereira EMV, Cavalcante GHF, Vieira LCM, Siqueira GH. Seismic fragility assessment for a RC building in seismically stable Brazil: A sensitivity analysis. J Build Eng 2022;60:105184. https://doi.org/10.1016/j.jobe.2022.105184.

[60] Remo JWF, Pinter N. Hazus-MH earthquake modeling in the central USA. Nat Hazards 2012;63:1055–81. https://doi.org/10.1007/s11069-012-0206-5.

[61] Bendito A, Rozelle J, Bausch D. Assessing Potential Earthquake Loss in Mérida State, Venezuela Using Hazus. Int J Disaster Risk Sci 2014;5:176–91. https://doi.org/10.1007/s13753-014-0027-0.

[62] Levi T, Bausch D, Katz O, Rozelle J, Salamon A. Insights from Hazus loss estimations in Israel for Dead Sea Transform earthquakes. Nat Hazards 2015;75:365–88. https://doi.org/10.1007/s11069-014-1325-y.

[63] Ploeger SK, Atkinson GM, Samson C. Applying the HAZUS-MH software tool to assess seismic risk in downtown Ottawa, Canada. Nat Hazards 2010;53:1–20. https://doi.org/10.1007/s11069-009-9408-x.

[64] Barbat AH, Pujades LG, Lantada N. Seismic damage evaluation in urban areas using the capacity spectrum method: Application to Barcelona. Soil Dyn Earthq Eng 2008;28:851–65. https://doi.org/10.1016/j.soildyn.2007.10.006.

[65] Lantada N, Pujades LG, Barbat AH. Vulnerability index and capacity spectrum based methods for urban seismic risk evaluation. A comparison. Nat Hazards 2009;51:501–24. https://doi.org/10.1007/s11069-007-9212-4.

[66] Gulati B. Earthquake Risk Assessment of Buildings: Applicability of HAZUS in Dehradun, India 2006:112.